

Binary black hole merger: symmetry and the spin expansion

Latham Boyle, Michael Kesden and Samaya Nissanke
*Canadian Institute for Theoretical Astrophysics (CITA), University of Toronto,
 60 St. George Street, Toronto, Ontario, M5S 3H8, Canada*
 (Dated: September 2007)

We regard binary black hole (BBH) merger as a map from a simple initial state (two Kerr black holes, with dimensionless spins \mathbf{a} and \mathbf{b}) to a simple final state (a Kerr black hole with mass m , dimensionless spin \mathbf{s} , and kick velocity \mathbf{k}). By expanding this map around $\mathbf{a} = \mathbf{b} = 0$ and applying symmetry constraints, we obtain a simple formalism that is remarkably successful at explaining existing BBH simulations. It also makes detailed predictions and suggests a more efficient way of mapping the parameter space of binary black hole merger. Since we rely on symmetry rather than dynamics, our expansion complements previous analytical techniques.

In binary black hole (BBH) merger, two black holes A and B (with masses M_a, M_b , and spins \mathbf{a}, \mathbf{b}) inspiral due to the emission of gravitational radiation and eventually merge to form a final black hole with mass m , spin vector \mathbf{s} , and recoil (or “kick”) velocity \mathbf{k} . How do the final quantities $\{m, \mathbf{k}, \mathbf{s}\}$ depend on the initial quantities $\{M_a, M_b, \mathbf{a}, \mathbf{b}\}$? This is a classic problem in general relativity (GR), with important implications for astrophysics, cosmology and gravitational wave (GW) detection. For example, when two galaxies merge, their central supermassive black holes also merge. The final quantities $\{m, \mathbf{k}, \mathbf{s}\}$ from these supermassive BBH mergers are linked (see [1] and references therein) to a variety of astrophysical observables including: (i) the quasar luminosity function; (ii) the location of quasars relative to their host galaxies; (iii) the orientation and shape of jets in active galactic nuclei; (iv) the correlation between black hole mass and velocity dispersion in the surrounding stellar bulge; (v) the density profile in galactic centers. The quantities $\{m, \mathbf{k}, \mathbf{s}\}$ are also intimately related to the spectrum of quasi-normal ringdown modes after BBH merger — a key observable for probing black holes and strong-field GR with GW detectors.

Following recent numerical breakthroughs [2, 3, 4], a number of groups can now simulate entire BBH mergers. In particular, they can choose a set of initial quantities $\{M_a, M_b, \mathbf{a}, \mathbf{b}\}$ and compute the corresponding final quantities $\{m, \mathbf{k}, \mathbf{s}\}$. As more of these extremely time-intensive simulations have gradually accumulated, certain patterns and trends have emerged. In previous work, some of these patterns have been described by empirical fitting functions [5, 6] which are loosely inspired by (but not derived from) post-Newtonian formulae [7]. In this paper, we show how these same patterns (and others) may in fact be derived from elementary symmetry arguments. This perspective has several advantages which make it complementary to post-Newtonian and numerical techniques. As we shall explain, the resulting formalism: (i) provides a simple conceptual understanding of BBH merger, accessible to non-experts; (ii) makes a host of new and derived predictions which go beyond the fitting formulae [5, 6]; (iii) suggests an efficient way to map out the parameter space of BBH mergers with simulations; and (iv) provides a map $\{M_a, M_b, \mathbf{a}, \mathbf{b}\} \rightarrow \{m, \mathbf{k}, \mathbf{s}\}$

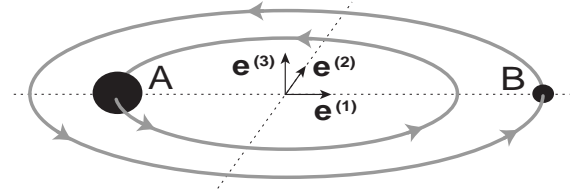


FIG. 1: The orthonormal triad presented in the text.

which is useful for astrophysical applications (including semi-analytic models or N-body simulations of black hole growth in galaxy mergers and dense stellar clusters) which wish to include BBH mergers, but cannot hope to follow the detailed merger dynamics.

Although the merger process involves complicated non-linear dynamics, the initial and final states of the system are rather simple and symmetric. The initial state consists of two widely separated Kerr black holes, and the final state is a single Kerr black hole. The idea of this *Letter* is to see how much we can learn by considering the merger process as a map between these simple initial and final states, ignoring as much as possible the detailed dynamics in between. Under three operations (rotation “ R ,” parity “ P ,” and exchange “ X ”), the initial and final states transform according to simple rules. The dependence of the final state on the initial state is constrained to be consistent with these rules. We present a naive formalism based on systematically applying these symmetry considerations to a well chosen Taylor expansion.

Imagine two black holes, A and B , in a circular orbit [17]. The orbit gradually shrinks due to gravitational-wave emission, until A and B eventually merge. Consider an initial instant when the holes are far apart — far enough that they may be approximated as two Kerr black holes with well defined masses (M_a and M_b) and dimensionless spins ($\mathbf{a} \equiv \mathbf{S}_a/M_a^2$ and $\mathbf{b} \equiv \mathbf{S}_b/M_b^2$), orbiting in a well defined plane that is perpendicular to the initial (dimensionless) orbital angular momentum \mathbf{L}_0/M^2 (where $M = M_a + M_b$, and $G_N = c = 1$). Long after the merger is complete, the gravitational radiation has total energy E_{rad} and total angular momentum \mathbf{J}_{rad} ; and the final Kerr black hole has dimensionless mass $m = M_f/M$,

dimensionless kick velocity \mathbf{k} (relative to the center of mass), and dimensionless spin $\mathbf{s} = \mathbf{S}_f/M_f^2$.

At the initial instant mentioned above, we define an orthonormal triad $\{\mathbf{e}^{(1)}, \mathbf{e}^{(2)}, \mathbf{e}^{(3)}\}$ as shown in Fig. 1: $\mathbf{e}^{(3)}$ is the direction of the orbital angular momentum, $\mathbf{e}^{(1)}$ is the direction from A to B , and $\mathbf{e}^{(2)} = \mathbf{e}^{(3)} \times \mathbf{e}^{(1)}$. Then the circular BBH's initial state is specified by 7 numbers: the mass ratio q and the spin components

$$a_i = \mathbf{a} \cdot \mathbf{e}^{(i)} \quad b_i = \mathbf{b} \cdot \mathbf{e}^{(i)} \quad (1)$$

relative to the orthonormal triad. Similarly, let us convert the final vectors into their separate triad components

$$k_i = \mathbf{k} \cdot \mathbf{e}^{(i)} \quad s_i = \mathbf{s} \cdot \mathbf{e}^{(i)}. \quad (2)$$

If we apply a global 3-dimensional rotation R to the entire binary system (as if it were a single rigid body), initial and final quantities like \mathbf{a} , \mathbf{b} , \mathbf{k} , and \mathbf{s} rotate as vectors — as do the triad elements $\mathbf{e}^{(i)}$. Therefore, the corresponding triad components (a_i , b_i , k_i , and s_i) transform as *scalars* under R . By working with triad components, all of our subsequent formulae are manifestly consistent with rigid 3-dimensional rotations R .

We can view any final quantity f (such as m , s_i , or k_i) as a function of the initial quantities:

$$f = f(q, a_1, a_2, a_3, b_1, b_2, b_3). \quad (3)$$

Let us Taylor expand this function around $\mathbf{a} = \mathbf{b} = 0$:

$$f = f^{m_1 m_2 m_3 | n_1 n_2 n_3}(q) a_1^{m_1} a_2^{m_2} a_3^{m_3} b_1^{n_1} b_2^{n_2} b_3^{n_3}. \quad (4)$$

Since a Kerr black hole has maximum spin $\mathbf{S}_i \leq M_i^2$, $|\mathbf{a}|$ and $|\mathbf{b}|$ are both ≤ 1 and it is not unreasonable to hope that the Taylor series might be convergent over most or even all of this range of initial spins.

We will now use additional symmetries to restrict the coefficients in this expansion. First consider a parity transformation P that reflects every point of the binary system through the origin (the center of mass). Under P , the mass ratio q is unchanged, while the triad components transform as

$$\begin{aligned} \{a_1, a_2, a_3\} &\rightarrow \{-a_1, -a_2, a_3\} \\ \{b_1, b_2, b_3\} &\rightarrow \{-b_1, -b_2, b_3\} \end{aligned} \quad (5)$$

Thus, each term on the right-hand-side of Eq. (4) picks up a factor of $(-1)^\gamma$, where

$$\gamma = m_1 + m_2 + n_1 + n_2. \quad (6)$$

If f transforms under P as $f \rightarrow (\pm)_P f$, the coefficients in Eq. (4) must satisfy the constraint

$$f^{m_1 m_2 m_3 | n_1 n_2 n_3}(q) = (\pm)_P (-1)^\gamma f^{m_1 m_2 m_3 | n_1 n_2 n_3}(q). \quad (7)$$

In other words, if f is even (odd) under P , then $f^{m_1 m_2 m_3 | n_1 n_2 n_3}(q)$ must vanish when γ is odd (even).

Finally, we apply an “exchange transformation” X . This leaves the physical system absolutely unchanged,

f	$m, E^{\text{rad}}, s_3, J_3^{\text{rad}}$	$s_1, s_2, J_1^{\text{rad}}, J_2^{\text{rad}}$	k_1, k_2	k_3
$(\pm)_P$	+	−	+	−
$(\pm)_X$	+	−	−	+
$(\pm)_{PX}$	+	+	−	−

TABLE I: Transformation under P , X , and PX , for various final quantities f .

and simply swaps the labels of the two black holes, $A \leftrightarrow B$. Under X , the mass ratio transforms as $q \rightarrow 1/q$, while the triad components transform as

$$\begin{aligned} \{a_1, a_2, a_3\} &\rightarrow \{-b_1, -b_2, b_3\} \\ \{b_1, b_2, b_3\} &\rightarrow \{-a_1, -a_2, a_3\} \end{aligned} \quad (8)$$

If f transforms under X as $f \rightarrow (\pm)_X f$, the coefficients in Eq. (4) must satisfy the constraint

$$f^{m_1 m_2 m_3 | n_1 n_2 n_3}(q) = (\pm)_X (-1)^\gamma f^{n_1 n_2 n_3 | m_1 m_2 m_3}(1/q). \quad (9)$$

Equivalently, and more conveniently, if f transforms under PX (P followed by X , or vice versa) as $f \rightarrow (\pm)_{PX} f$, the coefficients in Eq. (4) must satisfy the constraint

$$f^{m_1 m_2 m_3 | n_1 n_2 n_3}(q) = (\pm)_{PX} f^{n_1 n_2 n_3 | m_1 m_2 m_3}(1/q). \quad (10)$$

The transformation laws under P , X , and PX , for various final quantities f , are summarized in Table I.

Eqs. (4, 7, 10) imply a number of results that are *exact* (i.e. valid to all order in the Taylor expansion). For example, if the initial spin configuration has $\mathbf{a} \propto \mathbf{b} \propto \mathbf{e}^{(3)}$, then $\gamma = 0$ and parity requires $\mathbf{s} \propto \mathbf{e}_3$ and $k_3 = 0$. In the equal-mass case, $q = 1 = 1/q$ and Eq. (10) demands that all final quantities odd under PX (like k_i) vanish for $\mathbf{a} = \mathbf{b}$. Again in the equal-mass case, if the initial spin configuration satisfies $(a_1, a_2, a_3) = (-b_1, -b_2, b_3)$, then Eq. (8) becomes the identity mapping and all quantities odd under X (like s_1, s_2, k_1, k_2) must vanish.

Although these exact results are interesting, the real power of our formalism lies in the many *approximate* predictions that it makes. To illustrate this, consider the quantity k_1 . From Table I, k_1 has $(\pm)_P = +1$ and $(\pm)_{PX} = -1$. Start from the general Taylor expansion:

$$k_1 = k_1^{m_1 m_2 m_3 | n_1 n_2 n_3} a_1^{m_1} a_2^{m_2} a_3^{m_3} b_1^{n_1} b_2^{n_2} b_3^{n_3}. \quad (11)$$

The zeroth-order term $k_1^{000|000}$ vanishes by Eq. (10). At first order, the Taylor expansion has six terms (one for each of the spin components $\{a_1, a_2, a_3, b_1, b_2, b_3\}$). But constraints (7) and (10) cut this down to a single term:

$$k_1 = k_1^{001|000} (a_3 - b_3). \quad (12)$$

Thus, at leading order, we predict $k_1 \propto (a_3 - b_3)$, a trend seen in simulations. But we also predict that this leading-order behavior should be corrected by quadratic terms of a specific form. Although the naive Taylor expansion

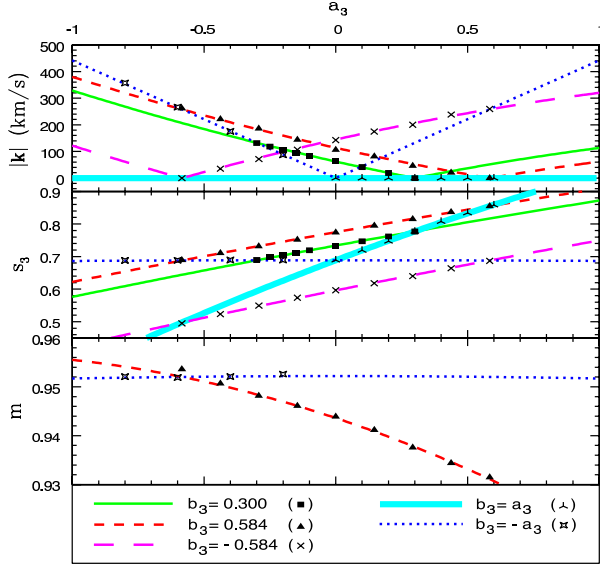


FIG. 2: Equal-mass BBHs with $\mathbf{a} \propto \mathbf{b} \propto \mathbf{e}^{(3)}$. Final kick $|\mathbf{k}|$, spin s_3 , and mass m are plotted versus a_3 . The five curves in the top two panels correspond to the five simulation sequences in [10]; within each sequence b_3 takes on the values shown in the bottom panel as a_3 is varied. For presentation purposes we have exchanged a_3 and b_3 for the case $b_3 = -0.584$. Cross and triangle data points for the mass m are taken from [11] and [12], respectively.

contains 21 new terms at 2nd order in spin, Eqs. (7) and (10) reduce this to only 5 new terms, yielding the general 2nd-order formula

$$k_1 = k_1^{001|000}(a_3 - b_3) + k_1^{002|000}(a_3^2 - b_3^2) + k_1^{200|000}(a_1^2 - b_1^2) + k_1^{110|000}(a_1 a_2 - b_1 b_2) + k_1^{020|000}(a_2^2 - b_2^2) + k_1^{100|010}(a_1 b_2 - b_1 a_2). \quad (13)$$

This expansion could be continued to 3rd order and beyond. At each order, we obtain more terms — although far fewer than a naive Taylor expansion would suggest.

Our symmetry arguments are unable to determine the numerical values of the 6 coefficients ($k_1^{001|000}$, etc.) in Eq. (13). These coefficients must be calibrated by 6 equal-mass simulations with independent initial spin configurations. If each simulation measures a reliable value for k_1 , we can simply *solve* for these coefficients. Each of these simulations should be performed at a fixed value of some inspiral parameter (such as the orbital separation r_0 or angular momentum L_0) which monotonically varies as the orbit shrinks. Having determined the coefficients, one can *predict* (with 2nd-order accuracy) the value of k_1 resulting from *any* arbitrary configuration of the initial spins at the *same* fixed value of the inspiral parameter. Post-Newtonian methods [7] can then relate coefficients determined at other fixed inspiral parameter values [9].

Similar arguments to those given in the k_1 example apply to any final quantity f , including the final mass

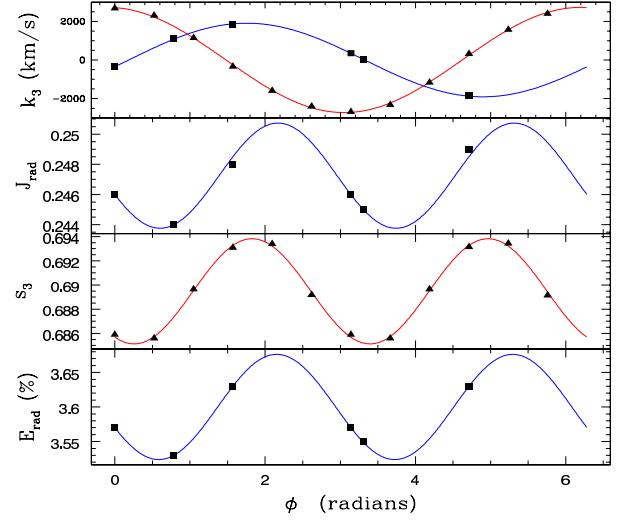


FIG. 3: Equal-mass BBHs with equal and opposite spins lying in the orbital plane. Kick velocity k_3 , radiated angular momentum J_{rad} , final spin s_3 , and percentage of radiated energy E_{rad} are plotted against the angle ϕ between the initial spin \mathbf{a} and $\mathbf{e}^{(1)}$. The blue curves show fits to the square data points taken from [13], while the red curves show fits to the triangle data points of [14].

m , and the magnitude and components of \mathbf{k} and \mathbf{s} .

The explanatory power of this “spin expansion” formalism is illustrated by a few simple examples. (For more details, we refer the reader to a subsequent paper [9], in which we discuss the formalism’s new predictions in more depth, and test them in detail against currently available simulations.) We begin with the case of equal-mass BBHs with spins aligned or anti-aligned with \mathbf{L}_0 (*i.e.* $\mathbf{a} \propto \mathbf{b} \propto \mathbf{e}^{(3)}$). Expanding the final kick k_i to 2nd-order in initial spins yields 3 terms for $|\mathbf{k}|^2$, and 4 terms each for the final spin s_3 , and mass m [18]. Fig. 2 shows our best fits for this configuration. As seen in the figure, the data are well-described by the linear terms in the spin expansion, and the fits also show evidence for small second order corrections of the predicted form.

Fig. 3 shows our fits for the “superkick” configuration (equal-mass BBHs with equal and opposite spins and $a_i = -b_i = a(\cos \phi, \sin \phi, 0)$). The leading-order terms in the spin expansion explain the previously noticed [13, 14] behavior $k_3 = Aa \cos(\phi - \phi_1)$ where A and ϕ_1 are constants (top panel in Fig. 3). Keeping terms to 2nd-order, the spin expansion also correctly predicts that the final quantities $f = \{J_{\text{rad}}, s_3, E_{\text{rad}}\}$ all behave as $f = B + Ca^2 \cos(2\phi - \phi_2)$, where B , C , and ϕ_2 are constants (bottom 3 panels in Fig. 3). This $\cos(2\phi - \phi_2)$ behavior highlights the power of the spin expansion to go beyond previous linear post-Newtonian fitting formulae to uncover and *explain* new and essentially non-linear behavior in the simulations.

Finally we examine the case of arbitrarily oriented initial spins. From each of the 8 simulations in [16] we have

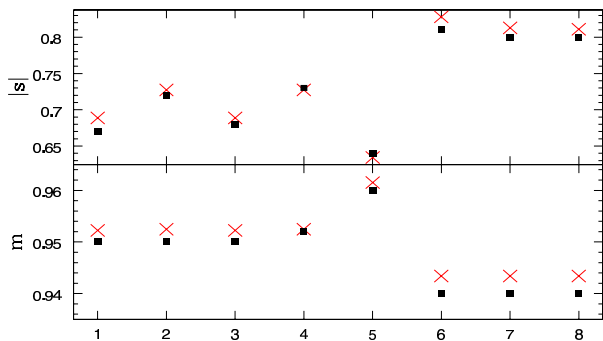


FIG. 4: Equal-mass BBHs with equal spin magnitudes and generic spin orientations. Square data points 1 through 8 indicate the final kick $|k|$, spin $|s|$, and mass m for eight simulations listed from left to right in Table I of [16]. Red X's show our predictions for these final quantities.

$|s|$ and m . We use the coefficients obtained from our fits in Fig. 2 for the terms that depend only on a_3 and b_3 . Then our 1st-order fits for $|s|$ (with 3 free parameters) and m (with *zero* free parameters!) are shown in Fig. (4). We stress that this data set is not described by any previous fitting formula. The spin expansion gives the first explanation for the distribution of points Fig. 4.

In this *Letter*, we introduce a new *spin expansion* of final quantities f in triad components a_i, b_i of the initial spins. Using the transformation properties of f , a_i , b_i and q under parity P and exchange X , we dramatically reduce the number of terms that one might naively expect. Without resorting to the sophisticated machinery of numerical relativity and the post-Newtonian expansion, we obtain some detailed (and often new) quantitative understanding of the final state of BBH merger. This clarifies the separation between the non-linear dynamics of Einstein's equations and our more elementary

non-dynamical considerations.

Our approach complements both post-Newtonian approximations and numerical relativity. Post-Newtonian methods provide accurate predictions in the weak-field inspiral regime, but break down during the later stages of the merger. By contrast, the symmetries under P and X implicitly hold through the entire merger.

Only numerical relativity can model the late stages of the merger, but simulations remain computationally expensive. The spin expansion offers enormous computational savings in mapping the 7-dimensional parameter space of BBH initial states $\{q, a_i, b_i\}$. Even 10 grid points along each direction would mean 10^7 simulations — a hopelessly large number. However, the values $\{m, k_i, s_i\}$ from 16 independent simulations determine the spin expansion coefficients up to 2nd order at fixed mass ratio q . Then, with 10 grid points for q , a mere 160 simulations could map the space $\{q, a_i, b_i\}$. Further reductions are possible if the q dependence of our coefficients can be identified analytically. The spin expansion may also help in identifying systematic errors with forbidden geometrical dependence on the initial spins.

The spin expansion is useful for astrophysics and cosmology — *e.g.* allowing BBH results from numerical relativity to be efficiently included in simulations of cosmological structure formation or black hole growth. These simulations cannot resolve the short scales relevant to supermassive BBH merger, and must instead rely on maps from the initial to final state such as those presented in this *Letter*. The spin expansion predicts these final quantities for *arbitrary* initial spin configurations, specified once gravitational radiation (rather than dynamical friction) dominates the binary evolution.

Acknowledgements. We thank Alessandra Buonanno, Neal Dalal, Larry Kidder, Luis Lehner, Eric Poisson, Harald Pfeiffer, Jonathan Sievers, Bill Unruh and Daniel Wesley for helpful conversations.

-
- [1] F. Pretorius, arXiv:0710.1338 [gr-qc].
 - [2] F. Pretorius, Phys. Rev. Lett. **95**, 121101 (2005).
 - [3] M. Campanelli *et al.*, Phys. Rev. Lett. **96**, 111101 (2006).
 - [4] J. G. Baker *et al.*, Phys. Rev. Lett. **96**, 111102 (2006).
 - [5] M. Campanelli *et al.*, Astrophys. J. **659**, L5 (2007).
 - [6] J. G. Baker *et al.*, Astrophys. J. **668**, 1140 (2007).
 - [7] L. Kidder, Phys. Rev. D **52**, 821 (1995).
 - [8] P. C. Peters and J. Mathews, Phys. Rev. **131**, 435 (1963).
 - [9] L. Boyle and M. Kesden, arXiv:0712.2819 [astro-ph].
 - [10] L. Rezzolla *et al.*, arXiv:0708.3999 [gr-qc].
 - [11] F. Herrmann *et al.*, Astrophys. J. **661**, 430-436 (2007).
 - [12] D. Pollney *et al.*, arXiv:0707.2559 [gr-qc].
 - [13] M. Campanelli *et al.*, Phys. Rev. Lett. **98**, 231102 (2007).
 - [14] B. Brügmann *et al.*, arXiv:0707.0135 [gr-qc].
 - [15] F. Herrmann *et al.*, Phys. Rev. D **76**, 084032 (2007).
 - [16] W. Tichy and P. Marronetti, Phys. Rev. D **76**, 061502 (2007).
 - [17] For most astrophysically relevant systems, elliptical BBH orbits are expected to circularize long before merger [8]. The elliptical case is treated in [9].
 - [18] A few days before our *Letter* appeared, [10] gave a related expansion for this special case $\mathbf{a} \propto \mathbf{b} \propto \mathbf{e}^{(3)}$.